doi:10.3788/gzxb20154401.0126001

光阑对偏振高斯-谢尔模型光束偏振特性的影响

刘钧,曹杏,高明,吕宏,巩蕾
(西安工业大学 光电工程学院 光电信息技术研究所,西安 710021)

摘 要:根据广义惠更斯-菲涅尔原理和 Collins 公式,基于复高斯函数展开法,推导出椭圆偏振的高斯-谢尔模型光束经过矩形光阑衍射后的交叉谱密度公式,结合斯托克斯矢量理论推导了椭圆偏振高斯-谢尔模型光束在接收平面的光强、偏振度、方位角和椭圆度的表达式,数值分析了光阑的孔径遮拦比对光强、偏振度及方位角和椭圆度的影响.结果表明,光阑的孔径遮拦比在近场区对经过光阑后椭圆偏振高斯-谢尔模型光束的光强和偏振特性有显著影响;随着传输距离的增大,光强和偏振特性受孔径遮拦比的影响减小,光强和偏振特性变化平稳.

关键词:光阑;孔径遮拦比;高斯-谢尔模型光束;椭圆偏振;传输与变换
中图分类号:TN249 **文献标识码**:A **文章编号**:1004-4213(2015)01-0126001-10

Effects of the Aperture on Polarization Properties of Polarized Gaussian Schell-model Beam

LIU Jun, CAO Xing, GAO Ming, LÜ Hong, GONG Lei
(*Institute of Optical Information Technology, School of Optoelectronic Engineering, Xi'an Technological University, Xi'an* 710021, *China*)

Abstract: According to the extended Huygens-Fresnel principle and Collins formula, based on complex Gaussian function expansion method, the cross-spectral density formula of elliptically polarized Gaussian Schell-model beam passing through the rectangular aperture was derived. Meanwhile combined the Stokes vector theory, the expressions of light intensity, the degree of polarization, the orientation angle and the degree of ellipticity on the receiver plane were studied. Furthermore, the effects of diaphragm aperture obscuration ratio on the light intensity, the degree of polarization, the orientation angle and the degree of ellipticity were analyzed. The results show that the light intensity and polarization properties of polarized Gaussian Schell-model beam passing through the aperture exhibit variation with oscillations, and effects of aperture obscuration ratio on them are drastic, especially in the near-field region. Besides, with the increasing of the transmission distance, effects of the aperture on the light intensity and polarization properties are reduced.

Key words: Aperture; Aperture obscuration ratio; Gaussian Schell-model beam; Elliptically polarized; Propagation and transformation
OCIS Codes: 260.5430; 140.3295; 050.1220; 220.2560

Foundation item: The Scientific Research Program Funded by Shaanxi Provincial Education Department (No. 14JK1350), the Natural Science Basic Research Plan in Shaanxi Province (Nos. 2012JM8008, 2013JQ8018), the National Natural Science Foundation of China (No. 61308071), the funded projects of the Natural Science Special of the Department of Education in Shaanxi Province (No. 2013JK0633), and the open foundation of Shaanxi Key Laboratory of Photoelectric Measurement and Instrument Technology
First author: LIU Jun (1964-), female, professor, M. S. degree, mainly focuses on photoelectric instrument design, optical design and the propagation and transformation of laser beams. Email:junliu1990@163.com
Corresponding author: CAO Xing (1988-), female, M. S. degree candidate, mainly focuses on optical design and the propagation and transformation of laser beams. Email:XingCaolove@126.com
Received: Jun. 10, 2014; **Accepted**: Sep. 3, 2014

0 Introduction

The propagation and transformation of the laser beam are frontal topics in the field of laser research. Polarization characteristics is an inherent characteristic of laser beam, which has an important significance on the application of laser technology[1-3]. Some optical systems have high demands on polarization properties of the beam, for instance, in polarization measurement, polarization imaging technology applications fields and so on, the polarization state of the light will affect the image contrast when large numerical aperture imaging. Making a qualitative and quantitative analysis to the polarization state of light beam passing through the optical system, can effectively improve the polarization effect problems presented in the optical system, so as to improve the performance of the entire optical system, which is a certain reference and guidance to optical design. In addition, in the optical design, the analysis to the energy of the incident light is a basic transmission requirement. However, the energy calculation methods are depend on the polarization states of the beam, and therefore research on the polarization state of the beam is an indispensable part for the light energy transmission in optical system. What′ s more, regulating the polarization state of the beam is expected to generate some new optical phenomenons or effects, extending and enhancing the performance of the traditional optical system. Recently, great progresses of the study of vector beam are achieved, especially in the field of beam generation, propagation and focusing, and interaction with other substances, which are expected to applied in the fields of optical microscopy, imaging, particle manipulation, optical trapping and materials processing[4-5].

As a better mathematical-physical model of partially coherent light, Gaussian Schell-Model beam (GSM) is depicted with mutual intensity in the space-time domain or cross-spectral density function in the space-frequency domain[6]. Recently, based on Collins integral formula, a number of researches have been carried out on all kinds of the beam propagation problems, which are in the absence of aperture or neglecting the aperture diffraction effects. JIA Xin-ting[7] studied the propagation characteristics of the axially symmetric polarized beam in free space under paraxial and non-paraxial approximation, and analyzed numerically the energy distribution of the beam under paraxial and non-paraxial approximation. ZHOU Zhe-hai[8] derived the mathematical expression of axisymmetric polarized beam in focus field of free space, and analyzed numerically intensity, phase and polarization distribution of different types of axisymmetric polarized light beam in focus field. In applications, the propagation of laser beam is often restricted by aperture, so the impact of aperture diffraction effects on the beam characteristics can not be ignored. Since professor Emil Wolf proposed the unified theory of coherence and polarization to uniformly study the spectrum, coherence, and polarization of the beam[9-11]. ZHAO Ting-jing[12] studied the axial polarization properties of GSM passing through an aperture, but the essay did not take the polarized GSM into account. PAN Liu-zhan[13] discussed the far-field characteristics of the partially polarized GSM passing through an aperture, however, the main method is just limited to scalar approximation theory.

In this paper, according to the extended Huygens-Fresnel principle and Collins formula, based on complex Gaussian function expansion method, the light intensity and polarization characteristics of elliptically polarized GSM diffracted by the aperture are calculated numerically. The effects of the aperture obscuration ratio and wavelength on the light intensity distribution are analyzed. Finally we discussed the effects of the aperture obscuration ratio and diffraction angle on the degree of polarization, orientation angle and degree of ellipticity.

1 Theoretical derivation

The cross-spectral density matrix of the elliptically polarized GSM across the input plane $z=0$ is given by[11]

$$\begin{bmatrix} \boldsymbol{W}_{xx} & \boldsymbol{W}_{xy} \\ \boldsymbol{W}_{yx} & \boldsymbol{W}_{yy} \end{bmatrix} \tag{1}$$

where

$$\boldsymbol{W}_{ij}(\boldsymbol{r}_1,\boldsymbol{r}_2,0)=A_iA_jB_{ij}\exp\left[-\left(\frac{\boldsymbol{r}_1^2}{4\sigma_i^2}+\frac{\boldsymbol{r}_2^2}{4\sigma_j^2}\right)\right]\cdot \exp\left[-\frac{(\boldsymbol{r}_2-\boldsymbol{r}_1)^2}{2\delta_{ij}^2}\right] \quad (i,j=x,y) \tag{2}$$

where vector $\boldsymbol{r}_1$ and $\boldsymbol{r}_2$ denote the position vectors of any two points across the input plane $z=0$, respectively.

In the Cartesian coordinate system, Eq. (2) can be expressed as

$$\boldsymbol{W}_{ij}(x_1,y_1,x_2,y_2,0)=A_iA_jB_{ij}\exp\left(-\frac{x_1^2+y_1^2}{4\sigma_i^2}-\frac{x_2^2+y_2^2}{4\sigma_j^2}\right)\cdot \exp\left[-\frac{(x_1-x_2)^2+(y_1-y_2)^2}{2\sigma_{ij}^2}\right] \tag{3}$$

where x and y refer to two mutually orthogonal directions across the input plane $z=0$, A_i and A_j are amplitudes, σ_i and σ_j are effective widths of the spectral density, respectively, B_{ij} is the phase correlation coefficient, δ_{ij} is the coherence length of the field.

When $|B_{xy}|=1$ and $\delta_{xx}=\delta_{yy}=\delta_{xy}$, GSM is fully polarized.

Using the Collins integral formula, elements of cross-spectral density matrix after GSM passing through the paraxial *ABCD* optical system obey the propagation law

$$\boldsymbol{W}_{ij}^{'}(x_1^{'},y_1^{'},x_2^{'},y_2^{'},z)=\frac{1}{(\lambda\boldsymbol{B})^2}\exp\left[-\frac{\mathrm{i}k\boldsymbol{D}}{2\boldsymbol{B}}(x_1^{'2}-x_2^{'2}+y_1^{'2}-y_2^{'2})\right]\times\iint\iint\boldsymbol{W}_{ij}(x_1,y_1,x_2,y_2,0)\cdot\exp\left\{-\frac{\mathrm{i}k}{2\boldsymbol{B}}[-2(x_1x_1^{'}-x_2x_2^{'}+y_1y_1^{'}-y_2y_2^{'})]\right\}\times\exp\left\{-\frac{\mathrm{i}k}{2\boldsymbol{B}}[\boldsymbol{A}(x_1^2-x_2^2+y_1^2-y_2^2)]\right\}\mathrm{d}x_1\mathrm{d}y_1\mathrm{d}x_2\mathrm{d}y_2 \tag{4}$$

where $k=2\pi/\lambda$ is the wave number, λ is wavelength, $\boldsymbol{A}$, $\boldsymbol{B}$ and $\boldsymbol{D}$ are *ABCD* matrix elements, and omits the constant phase factor.

Assume that there is a rectangular aperture with the half-width of a in both x and y directions. Considering Eq. (3), and after the calculation

$$\int_{-a}^{a}\int_{-a}^{a}\int_{-a}^{a}\int_{-a}^{a}\exp\left[-\frac{(x_1-x_2)^2+(y_1-y_2)^2}{2\delta_{ij}^2}\right]\cdot\mathrm{d}x_1\mathrm{d}y_1\mathrm{d}x_2\mathrm{d}y_2=\left\{4\left[\frac{1}{\exp(2a^2\delta_{ij}^2)}+\sqrt{2\pi}a\delta_{ij}\cdot\mathrm{erf}(\sqrt{2}a\delta_{ij})-1\right]^2\right\}/\delta_{ij}^4 \tag{5}$$

Eq. (4) can be written as

$$\begin{aligned}\boldsymbol{W}_{ij}^{'}(x_1^{'},y_1^{'},x_2^{'},y_2^{'},z)=&\frac{1}{(\lambda\boldsymbol{B})^2}A_iA_jB_{ij}\cdot\frac{\left[\frac{1}{\exp(2a^2\delta_{ij}^2)}+\sqrt{2\pi}a\delta_{ij}\,\mathrm{erf}(2a\delta_{ij})-1\right]^2}{\delta_{ij}^4}\cdot\exp\left[-\frac{\mathrm{i}k\boldsymbol{D}}{2\boldsymbol{B}}(x_1^{'2}-x_2^{'2}+y_1^{'2}-y_2^{'2})\right]\times\int_{-a}^{a}\int_{-a}^{a}\int_{-a}^{a}\int_{-a}^{a}\exp\left(-\frac{x_1^2+y_1^2}{4\sigma_i^2}-\frac{x_2^2+y_2^2}{4\sigma_j^2}\right)\exp\left\{-\frac{\mathrm{i}k}{2\boldsymbol{B}}[-2(x_1x_1^{'}-x_2x_2^{'}+y_1y_1^{'}-y_2y_2^{'})]\right\}\exp\left\{-\frac{\mathrm{i}k}{2\boldsymbol{B}}[\boldsymbol{A}(x_1^2-x_2^2+y_1^2-y_2^2)]\right\}\mathrm{d}x_1\mathrm{d}y_1\mathrm{d}x_2\mathrm{d}y_2\end{aligned} \tag{6}$$

In order to simplify the project, Eq. (6) can be rewritten as

$$\boldsymbol{W}_{ij}^{'}(x_1^{'},y_1^{'},x_2^{'},y_2^{'},z)=\boldsymbol{W}_{ij}^{'}(x_1^{'},y_1^{'},z)\boldsymbol{W}_{ij}^{'}(x_x^{'},y_x^{'},z) \tag{7}$$

where

$$\begin{aligned}\boldsymbol{W}_{ij}^{'}(x_1^{'},y_1^{'},z)=&\frac{-2\mathrm{i}}{\lambda\boldsymbol{B}}\sqrt{A_iA_jB_{ij}}\cdot\frac{1}{\exp(2a^2\delta_{ij}^2)}+\sqrt{2\pi}a\delta_{ij}\,\mathrm{erf}(2a\delta_{ij})-1}{\delta_{ij}^2}\cdot\exp\left\{-\frac{\mathrm{i}k\boldsymbol{D}}{2\boldsymbol{B}}[-(x_1^{'2}+y_1^{'2})]\right\}\int_{-a}^{a}\int_{-a}^{a}\exp\left\{-\frac{\mathrm{i}k}{2\boldsymbol{B}}[\boldsymbol{A}(x_1^2+y_1^2)]\right\}\mathrm{d}x_1\mathrm{d}y_1\end{aligned} \tag{8}$$

$$\begin{aligned}\boldsymbol{W}_{ij}^{'}(x_1^{'},y_1^{'},z)=&\frac{-2\mathrm{i}}{\lambda\boldsymbol{B}}\sqrt{A_iA_jB_{ij}}\cdot\frac{1}{\exp(2a^2\delta_{ij}^2)}+\sqrt{2\pi}a\delta_{ij}\,\mathrm{erf}(2a\delta_{ij})-1}{\delta_{ij}^2}\cdot\exp\left\{-\frac{\mathrm{i}k\boldsymbol{D}}{2\boldsymbol{B}}[-(x_2^{'2}+y_2^{'2})]\right\}\int_{-a}^{a}\int_{-a}^{a}\exp(-\frac{x_2^2+y_2^2}{4\sigma_i^2})\exp\left\{-\frac{\mathrm{i}k}{2\boldsymbol{B}}[2(x_2x_2^{'}+y_2y_2^{'})]\right\}\cdot\exp\left\{-\frac{\mathrm{i}k}{2\boldsymbol{B}}[-\boldsymbol{A}(x_2^2+y_2^2)]\right\}\mathrm{d}x_2\mathrm{d}y_2\end{aligned} \tag{9}$$

Then, Eqs. (8) and (9) can be rewritten in normalized coordinate form

$$\begin{aligned}\boldsymbol{W}_{ij}^{'}(\xi_1^{'},\eta_1^{'},z)=&\frac{-2\mathrm{i}}{\lambda B}\omega_0^2\sqrt{A_iA_jB_{ij}}\cdot\frac{1}{\exp(2\varepsilon^2\omega_0^2\delta_{ij}^2)}+\sqrt{2\pi}\varepsilon\omega_0\delta_{ij}\,\mathrm{erf}(2\varepsilon\omega_0\delta_{ij})-1}{\delta_{ij}^2}\cdot\exp\left[-\frac{\mathrm{i}k\boldsymbol{D}}{2\boldsymbol{B}}\left(\frac{z}{z_0}\right)^2(\xi_1^{'2}+\eta_1^{'2})\omega_0^2\right]\int_{-\varepsilon}^{\varepsilon}\int_{-\varepsilon}^{\varepsilon}\exp\left(-\frac{\xi_1^2+\eta_1^2}{4\sigma_i^2}\omega_0^2\right)\exp\left\{-\frac{\mathrm{i}k}{2\boldsymbol{B}}\frac{z}{z_0}[-2(\xi_1\xi_1^{'}+\eta_1\eta_1^{'})\omega_0^2]\right\}\exp\left\{-\frac{\mathrm{i}k}{2\boldsymbol{B}}[\boldsymbol{A}(\xi_1^2+\eta_1^2)w_0^2]\right\}\mathrm{d}\xi_1\mathrm{d}\eta_1\end{aligned} \tag{10}$$

$$\begin{aligned}\boldsymbol{W}_{ij}^{'}(\xi_2^{'},\eta_2^{'},z)=&\frac{-2\mathrm{i}}{\lambda\boldsymbol{B}}\omega_0^2\sqrt{A_iA_jB_{ij}}\cdot\frac{1}{\exp(2\varepsilon^2\omega_0^2\delta_{ij}^2)}+\sqrt{2\pi}\varepsilon\omega_0\delta_{ij}\,\mathrm{erf}(2\varepsilon\omega_0\delta_{ij})-1}{\delta_{ij}^2}\cdot\exp\left[-\frac{\mathrm{i}k\boldsymbol{D}}{2\boldsymbol{B}}\left(\frac{z}{z_0}\right)^2(\xi_2^{'2}+\eta_2^{'2})\omega_0^2\right]\int_{-\varepsilon}^{\varepsilon}\int_{-\varepsilon}^{\varepsilon}\exp\left(-\frac{\xi_2^2+\eta_2^2}{4\sigma_i^2}\omega_0^2\right)\exp\left\{-\frac{\mathrm{i}k}{2\boldsymbol{B}}\frac{z}{z_0}[2(\xi_2\xi_2^{'}+\eta_2\eta_2^{'})\omega_0^2]\right\}\exp\left\{-\frac{\mathrm{i}k}{2\boldsymbol{B}}[-\boldsymbol{A}(\xi_2^2+\eta_2^2)w_0^2]\right\}\mathrm{d}\xi_2\mathrm{d}\eta_2\end{aligned} \tag{11}$$

where ω_0 is the waist of the beam, $z_0=\pi\omega_0^2/\lambda$ is the Rayleigh length, $\varepsilon=a/\omega_0$ is the aperture obscuration ratio, there are

$$\begin{cases}\xi_1=x_1/\omega_0\\ \eta_1=y_1/\omega_0\\ \xi_2=x_2/\omega_0\\ \eta_2=x_2/\omega_0\end{cases}$$

for normalized coordinate, and

$$\begin{cases}\xi_1^{'}=\dfrac{x_1^{'}/\omega_0}{z/z_0}\\ \eta_1^{'}=\dfrac{y_1^{'}/\omega_0}{z/z_0}\\ \xi_2^{'}=\dfrac{x_2^{'}/\omega_0}{z/z_0}\\ \eta_2^{'}=\dfrac{y_2^{'}/\omega_0}{z/z_0}\end{cases}$$

for normalized diffraction angle.

Introduce the aperture function

$$T_1(\xi,\eta)=\begin{cases}1, & \xi^2+\eta^2<\varepsilon^2\\ 0, & \xi^2+\eta^2>\varepsilon^2\end{cases} \tag{12}$$

then, expand the aperture function into a finite sum of complex Gaussian functions[14]

$$T_2(\xi,\eta)=\sum_{n=1}^{N}\alpha_n\exp\left(-\beta_n\frac{\xi^2+\eta^2}{\varepsilon^2}\right) \tag{13}$$

where N is the number of the expansion, and when N is a limited number, the expansion is approximation, generally choosing $N=10$ and sufficient accuracy can be received. Simultaneously, the complex constants α_n and β_n can be obtained by optimization computation.

On substituting Eqs. (12) and (13) into Eq. (10), Eq. (10) can be expressed in the following alternative form

$$\begin{aligned}\boldsymbol{W}_{ij}'(\xi_1',\eta_1',z)=&\frac{-2\mathrm{i}}{\lambda\boldsymbol{B}}\omega_0^2\sqrt{A_iA_jB_{ij}}\cdot\\&\frac{1}{\exp(2\varepsilon^2\omega_0^2\delta_{ij}^2)}+\sqrt{2\pi}\varepsilon\omega_0\delta_{ij}\operatorname{erf}(2\varepsilon\omega_0\delta_{ij})-1}{\delta_{ij}^2}\cdot\\&\exp\left[-\frac{\mathrm{i}k\boldsymbol{D}}{2\boldsymbol{B}}\left(\frac{z}{z_0}\right)^2(\xi_1'^2+\eta_1'^2)\omega_0^2\right]\int_{-\infty}^{\infty}\int_{-\infty}^{\infty}\\&T_1(\xi_1,\eta_1)\exp\left[-\left(\frac{\omega_0^2}{4\sigma_i^2}+\frac{\mathrm{i}k\boldsymbol{A}\omega_0^2}{2\boldsymbol{B}}\right)\xi_1^2+2\frac{z}{z_0}\cdot\right.\\&\left.\frac{\mathrm{i}k\xi_1'\omega_0^2}{2\boldsymbol{B}}\xi_1\right]\exp\left[-\left(\frac{\omega_0^2}{4\sigma_i^2}+\frac{\mathrm{i}k\boldsymbol{A}\omega_0^2}{2\boldsymbol{B}}\right)\cdot\right.\\&\left.\eta_1^2+2\frac{z}{z_0}\frac{\mathrm{i}k\eta_1'\omega_0^2}{2\boldsymbol{B}}\eta_1\right]\mathrm{d}\xi_1\,\mathrm{d}\eta_1\end{aligned} \tag{14}$$

Introducing integral formula[15]

$$\int_{-\infty}^{\infty}\exp(-ax^2\pm2bx)=\sqrt{\frac{\pi}{a}}\exp\left(\frac{b^2}{a}\right) \tag{15}$$

Eq. (14) can be rewritten as

$$\begin{aligned}\boldsymbol{W}_{ij}'(\xi_1',\eta_1',z)=&\frac{-2\mathrm{i}}{\lambda\boldsymbol{B}}\omega_0^2\sqrt{A_iA_jB_{ij}}\cdot\\&\frac{1}{\exp(2\varepsilon^2\omega_0^2\delta_{ij}^2)}+\sqrt{2\pi}\varepsilon\omega_0\delta_{ij}\operatorname{erf}(2\varepsilon\omega_0\delta_{ij})-1}{\delta_{ij}^2}\cdot\\&\exp\left[-\frac{\mathrm{i}k\boldsymbol{D}}{2\boldsymbol{B}}\left(\frac{z}{z_0}\right)^2(\xi_1'^2+\eta_1'^2)\omega_0^2\right]\cdot\\&\sum_{n=1}^{N}\frac{\alpha_n\pi}{\frac{\omega_0^2}{4\sigma_i^2}+\frac{\mathrm{i}k\boldsymbol{A}\omega_0^2}{2\boldsymbol{B}}+\frac{\beta_n}{\varepsilon^2}}\exp\left[\frac{-(\xi_1'^2+\eta_1'^2)}{\frac{\omega_0^2}{4\sigma_i^2}+\frac{\mathrm{i}k\boldsymbol{A}\omega_0^2}{2\boldsymbol{B}}+\frac{\beta_n}{\varepsilon^2}}\right]\end{aligned} \tag{16}$$

do the same calculation to $\boldsymbol{W}_{ij}'(\xi_2',\eta_2',z)$, which is omitted here, then

$$\begin{aligned}\boldsymbol{W}_{ij}'(\xi_1',\eta_1',\xi_2',\eta_2',z)=&\frac{-4\omega_0^4}{(\lambda\boldsymbol{B})^2}A_iA_jB_{ij}\cdot\\&\frac{\left[\frac{1}{\exp(2\varepsilon^2\omega_0^2\delta_{ij}^2)}+\sqrt{2\pi}\varepsilon\omega_0\delta_{ij}\operatorname{erf}(2\varepsilon\omega_0\delta_{ij})-1\right]^2}{\delta_{ij}^4}\cdot\\&\exp\left[-\frac{\mathrm{i}k\boldsymbol{D}\omega_0^2}{2\boldsymbol{B}}\left(\frac{z}{z_0}\right)^2(\xi_1'^2+\eta_1'^2-\xi_2'^2-\eta_2'^2)\right]\cdot\\&\sum_{n=1}^{N}\sum_{m=1}^{N}\left\{\frac{\alpha_n\pi}{\frac{\omega_0^2}{4\sigma_i^2}+\frac{\mathrm{i}k\boldsymbol{A}\omega_0^2}{2\boldsymbol{B}}+\frac{\beta_n}{\varepsilon^2}}\exp\left[\frac{-(\xi_1'^2+\eta_1'^2)}{\frac{\omega_0^2}{4\sigma_i^2}+\frac{\mathrm{i}k\boldsymbol{A}\omega_0^2}{2\boldsymbol{B}}+\frac{\beta_n}{\varepsilon^2}}\right]\cdot\right.\\&\left.\frac{\alpha_m\pi}{\frac{\omega_0^2}{4\sigma_j^2}-\frac{\mathrm{i}k\boldsymbol{A}\omega_0^2}{2\boldsymbol{B}}+\frac{\beta_m}{\varepsilon^2}}\exp\left[\frac{-(\xi_2'^2+\eta_2'^2)}{\frac{\omega_0^2}{4\sigma_j^2}-\frac{\mathrm{i}k\boldsymbol{A}\omega_0^2}{2\boldsymbol{B}}+\frac{\beta_m}{\varepsilon^2}}\right]\right\}\end{aligned} \tag{17}$$

Defining $x_1'=x_2'=x'$ and $y_1'=y_2'=y'$, that is $\xi_1'=\xi_2'=\xi'$ and $\eta_1'=\eta_2'=\eta'$, elements of cross-spectral density matrix after the beam passing through the aperture can be gained in the form

$$\begin{aligned}\boldsymbol{W}_{ij}'(\xi',\eta',\xi',\eta',z)=&\frac{-4\omega_0^4}{(\lambda z)^2}A_iA_jB_{ij}\cdot\\&\frac{\left[\frac{1}{\exp(2\varepsilon^2\omega_0^2\delta_{ij}^2)}+\sqrt{2\pi}\varepsilon\omega_0\delta_{ij}\operatorname{erf}(2\varepsilon\omega_0\delta_{ij})-1\right]^2}{\delta_{ij}^4}\cdot\\&\sum_{n=1}^{N}\sum_{m=1}^{N}\left\{\frac{\alpha_n\pi}{\frac{\omega_0^2}{4\sigma_i^2}+\frac{\mathrm{i}k\omega_0^2}{2z}+\frac{\beta_n}{\varepsilon^2}}\exp\left[\frac{-(\xi'^2+\eta'^2)}{\frac{\omega_0^2}{4\sigma_i^2}+\frac{\mathrm{i}k\omega_0^2}{2z}+\frac{\beta_n}{\varepsilon^2}}\right]\cdot\right.\\&\left.\frac{\alpha_m\pi}{\frac{\omega_0^2}{4\sigma_j^2}-\frac{\mathrm{i}k\omega_0^2}{2z}+\frac{\beta_m}{\varepsilon^2}}\exp\left[\frac{-(\xi'^2+\eta'^2)}{\frac{\omega_0^2}{4\sigma_j^2}-\frac{\mathrm{i}k\omega_0^2}{2z}+\frac{\beta_m}{\varepsilon^2}}\right]\right\}\end{aligned} \tag{18}$$

Using the Stokes parameters, the degree of polarization P can be given by

$$P=\sqrt{\frac{\boldsymbol{S}_1^2+\boldsymbol{S}_2^2+\boldsymbol{S}_3^2}{\boldsymbol{S}_0^2}} \tag{19}$$

where

$$\begin{cases}\boldsymbol{S}_0=\boldsymbol{W}_{xx}'+\boldsymbol{W}_{yy}'\\ \boldsymbol{S}_1=\boldsymbol{W}_{xx}'-\boldsymbol{W}_{yy}'\\ \boldsymbol{S}_2=\boldsymbol{W}_{xy}'+\boldsymbol{W}_{yx}'\\ \boldsymbol{S}_3=\mathrm{i}(\boldsymbol{W}_{yx}'-\boldsymbol{W}_{xy}')\end{cases} \tag{20}$$

Light intensity can be described by Stokes parameters

$$I=S_0 \tag{21}$$

Polarization characteristics of the beam can not be completely described by the degree of polarization, therefore it is necessary to introduce the orientation angle θ and the degree of ellipticity υ to further illustrate it[16]. Orientation angle θ is defined as the angle between the long axis and the axis x, which represents the orientation of the vibration ellipse, and its expression is

$$\theta=\frac{1}{2}\arctan\left[\frac{2\operatorname{Re}(\boldsymbol{W}_{xy}')}{\boldsymbol{W}_{xx}'-\boldsymbol{W}_{yy}'}\right] \tag{22}$$

The degree of ellipticity υ is defined as the ratio of the amplitude of the minor axis and the semi-major axis of the ellipse, which characterize the shape of the vibration ellipse, whose expression is

$$\upsilon=\frac{A_S}{A_M} \tag{23}$$

where

$$\begin{aligned}A_S^2=&\frac{1}{2}(\sqrt{(\boldsymbol{W}_{xx}'-\boldsymbol{W}_{yy}')^2+4|\boldsymbol{W}_{yy}'|^2}-\\&\sqrt{(\boldsymbol{W}_{xx}'-\boldsymbol{W}_{yy}')^2+4[\operatorname{Re}(\boldsymbol{W}_{xy}')]^2})\end{aligned} \tag{24}$$

$$\begin{aligned}A_M^2=&\frac{1}{2}(\sqrt{(\boldsymbol{W}_{xx}'-\boldsymbol{W}_{yy}')^2+4|\boldsymbol{W}_{yy}'|^2}+\\&\sqrt{(\boldsymbol{W}_{xx}'-\boldsymbol{W}_{yy}')^2+4[\operatorname{Re}(\boldsymbol{W}_{xy}')]^2})\end{aligned} \tag{25}$$

and then the degree of ellipticity υ is expressed as

$$\upsilon=[\sqrt{(\boldsymbol{W}_{xx}-\boldsymbol{W}_{yy})^2+4|\boldsymbol{W}_{xy}|^2}-\sqrt{(\boldsymbol{W}_{xx}-\boldsymbol{W}_{yy})^2+4[\mathrm{Re}(\boldsymbol{W}_{xy})]^2}]/[2\sqrt{|\boldsymbol{W}_{xx}|^2-[\mathrm{Re}(\boldsymbol{W}_{xy})]^2}] \quad (26)$$

According to the theoretical derivation above , the numerical simulation can be carried out.

2 Numerical simulation

Choose the beam with the parameters as follows, the waist of the beam $\omega_0=1$ mm, the ratio of the amplitude of electric field $A_x/A_y=1/2$, the phase correlation factorand $B_{xx}=B_{yy}=1$ and $B_{xy}=B_{yx}^*=\exp(\mathrm{i}\pi/3)$, the coherence length $\delta_{xx}=\delta_{yy}=\delta_{xy}=\delta_{yx}=2$ mm, meanwhile assume a anisotropic beam with the effective width of the spectral density $\sigma_x=1$ cm and $\sigma_y=2$ cm.

2.1 Effects of the aperture obscuration ratio and wavelength on light intensity

The numerical results for behaviour of light intensity with the transmission distance in different aperture obscuration ratios are complied in Fig. 1, where the wavelength $\lambda=1.06$ μm, diffraction angle $\xi'=1$, aperture obscuration ratios $\varepsilon=0.3$, 1, 3 and 5. As shown in Fig. 1, the variation of light intensity is not monotonous, especially in the near field zone. The light intensity exhibits decrement with oscillations and the oscillation is stronger for larger aperture obscuration ratios. Effects of aperture obscuration ratios on light intensity are drastic in the near field zone, and the variation of light intensity with the transmission distance is not obvious when $\varepsilon=0.3$. With the increasing of aperture obscuration ratio, the diffraction effects become apparent. So the variation of light intensity occurs at $\varepsilon=1$ and it becomes severe with the increasing of aperture obscuration ratio. When $\varepsilon=5$, the variation reaches to maximum. With the increasing of transmission distance, because the energy of the beam is weaken, the intensity distribution is invariant and no longer affected by the aperture obscuration ratio.

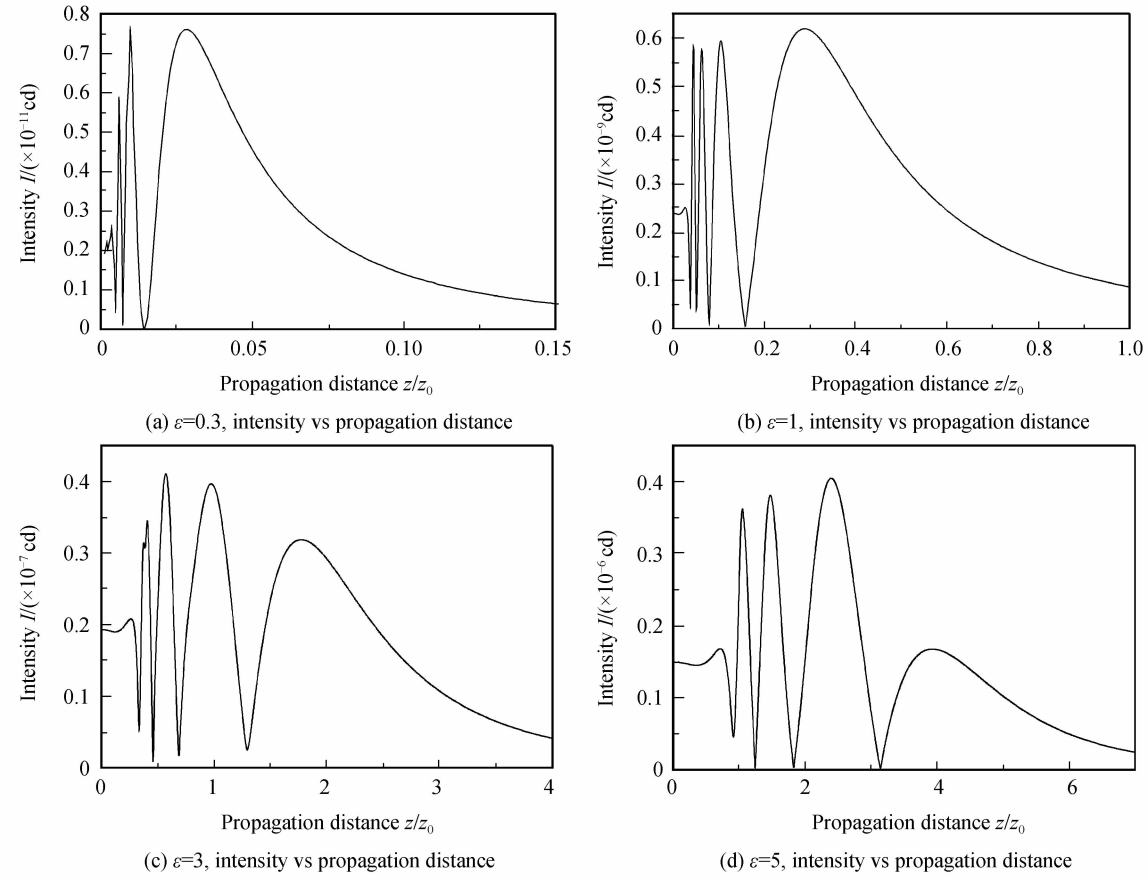

Fig. 1 Changes in light intensity with the transmission distance in different aperture obscuration ratios

The numerical results for behaviour of light intensity with the transmission distance in different wavelengths are shown in Fig. 2, where the aperture obscuration ratios $\varepsilon=1$, the diffraction angle $\xi'=1$, the wavelengths $\lambda=1.06$ μm, 3.8 μm and 10.6 μm. From Fig. 2 we can see that the variation of light intensity is not monotonous. The light intensity exhibits decrement with oscillations and the oscillation is stronger for larger wavelengths in the near field zone. It is clear that effects of wavelengths on the light intensity are

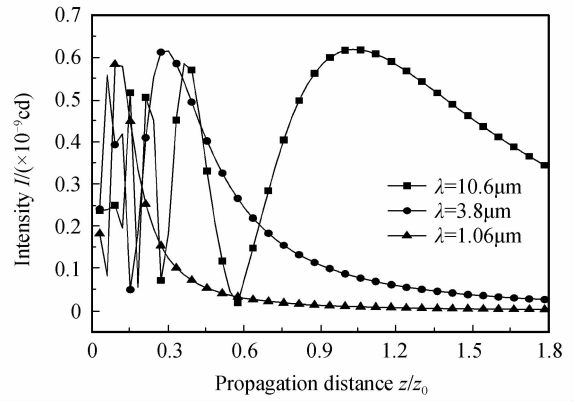

Fig. 2 Changes in light intensity with the transmission distance in different wavelengths

drastic in the near field zone, and variation of light intensity with the transmission distance is small at $\lambda=1.06$ μm. What's more, variation of light intensity become big when $\lambda=3.8$ μm and the effects of wavelengths on light intensity aggravate. That is because that the significant degree of diffraction phenomenon is closely related to the ratio of the wavelength λ and the aperture size a, and the diffraction phenomenon increases as the ratio λ/a increases. With the increasing of transmission distance, because the energy of the beam is weaken, the intensity distribution is no longer affected by the wavelength.

2.2 Effects of the aperture obscuration ratio and diffraction angle on polarization properties

2.2.1 *Effects of the aperture obscuration ratio and diffraction angle on the degree of polarization with the increasing of transmission distance*

The numerical results for behaviour of the degree of polarization with the transmission distance in different aperture obscuration ratios are given in Fig. 3, where the wavelengths $\lambda=1.06$ μm, the diffraction angle $\xi'=3$, the aperture obscuration ratios $\varepsilon=0.3$, 1, 3 and 5. As can be seen from Fig. 3, the larger the aperture obscuration is, the greater the degree of polarization will be. The variation of degree of polarization is not monotonous, and the degree of polarization exhibits growth with oscillations in the near field zone, meanwhile the oscillation is stronger for larger aperture obscuration ratios. It is easy to find that effects of aperture obscuration ratios on the degree of polarization are drastic in the near field zone. Moreover, the variation of the degree of polarization with the transmission distance is not obvious when $\varepsilon=0.3$. In addition, the variation of the degree of polarization appears at $\varepsilon=1$ and it becomes severe with the increasing of aperture obscuration ratio .

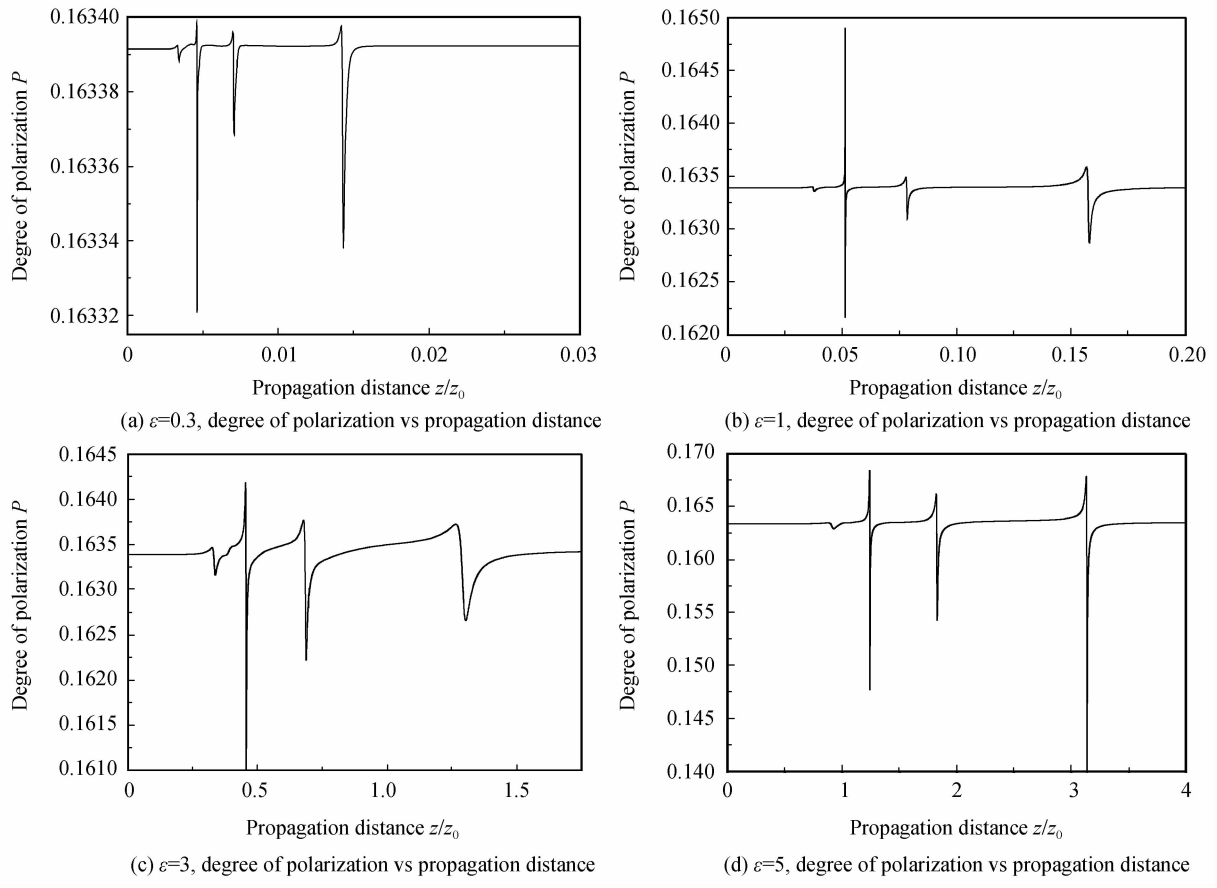

Fig. 3 Changes in the degree of polarization with the transmission distance in different aperture obscuration ratios

Furthermore, the variation with the transmission distance reaches to maximum when $\varepsilon = 5$. That is because that with the increasing of aperture obscuration ratio, the diffraction effects become apparent. With the increasing of transmission distance, because the energy of the beam is weaken, the degree of polarization is no longer affected by the aperture obscuration ratio.

Fig. 4 gives the behaviour of the degree of polarization with the transmission distance in different diffraction angles, where the wavelength $\lambda = 1.06$ μm,

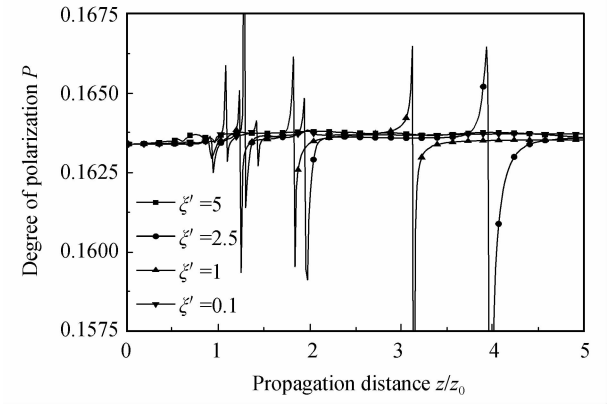

Fig. 4 Changes in the degree of polarization with the transmission distance in different diffraction angles

the aperture obscuration ratios $\varepsilon = 5$, the diffraction angles $\xi' = 0.1$, 1, 2.5 and 5. From Fig. 4, we can note that the variation of degree of polarization is not monotonous and the degree of polarization exhibits variation with oscillations, especially in the near field zone. It is easy to find that effects of diffraction angles on the degree of polarization are drastic in the near field zone, and variation of the degree of polarization with the transmission distance is not obvious when $\xi' = 0.1$. Furthermore, the variation of the degree of polarization becomes severe at $\xi' = 1$, and the variation reaches to maximum when $\xi' = 5$. That is because that dependence of the degree of polarization on spatial orientation is waned. In this case, the diffraction phenomenon becomes irregular, and then the oscillation is great. With the increasing of transmission distance, the variation of the degree of polarization becomes stable.

2.2.2 *Effects of the aperture obscuration ratio and diffraction angle on the orientation angle with the increasing of transmission distance*

The numerical results for variation of the orientation angle with the transmission distance in different aperture obscuration ratios are given in Fig. 5, where the wavelengths $\lambda = 1.06$ μm, the diffraction angle $\xi' = 2.5$, the aperture obscuration ratios $\varepsilon = 0.3$, 1, 3 and 5. Fig. 5 indicates that the variation of the orientation angle is not monotonous . The orientation

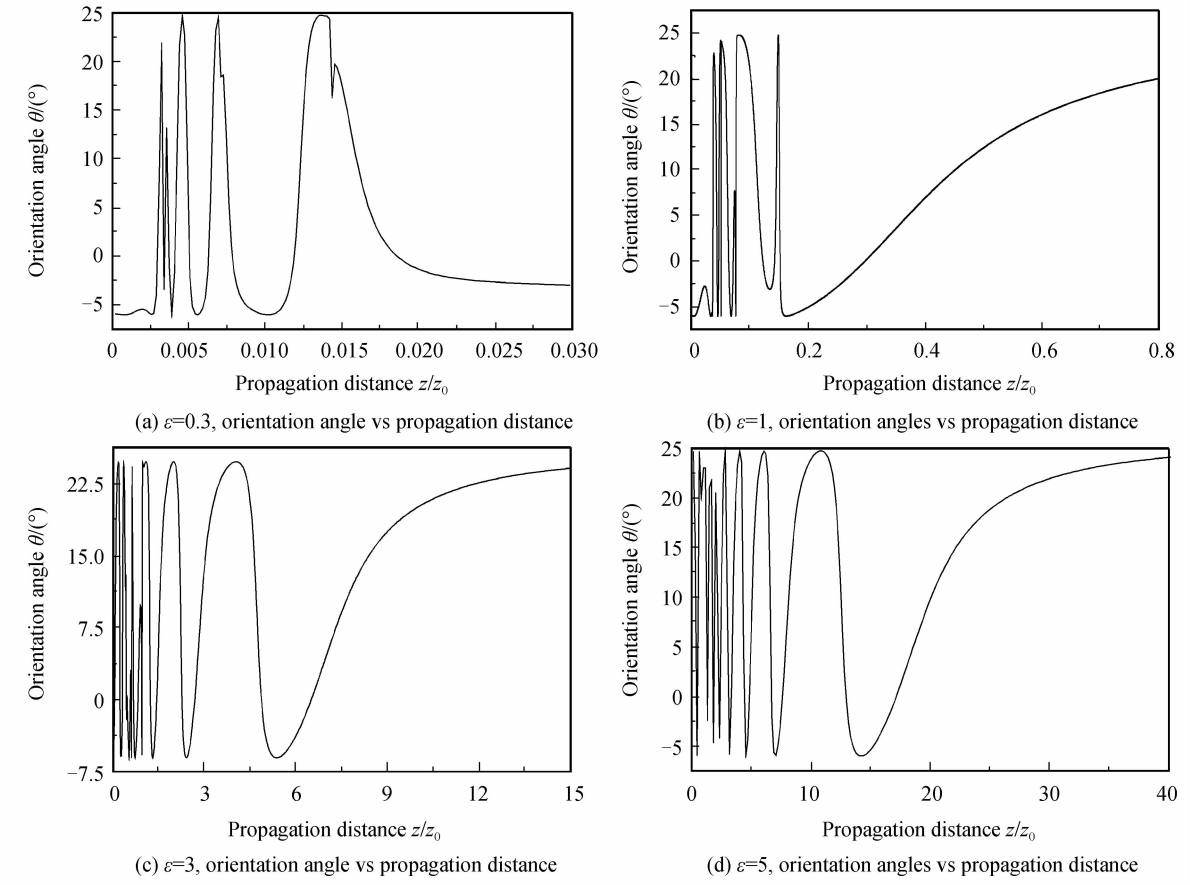

Fig. 5 Changes in the orientation angles with the transmission distance in different aperture obscuration ratios

angle exhibits decrement with oscillations and the oscillation is stronger for larger aperture obscuration ratios. Effects of aperture obscuration ratios on the orientation angle are drastic in the near field zone, and the variation of the orientation angle with transmission distance is not obvious when $\varepsilon=0.3$. Obviously, with the increasing of aperture obscuration ratio, the diffraction effects become apparent. The variation of orientation angles appears at $\varepsilon=1$ and it becomes severe with the increasing of aperture obscuration ratio. Furthermore, the variation reaches to maximum when $\varepsilon=5$. With the increasing transmission distance, due to the energy of the beam is weaken, the orientation angle is no longer affected by the aperture obscuration ratio and approaches a fixed value. That is because that the orientation angle is another expression of the degree of polarization, and it will change with the variation of the degree of polarization change.

Fig. 6 gives the behaviour of the orientation angle with the transmission distance in different diffraction angles, where the wavelength $\lambda=1.06$ μm, the aperture obscuration ratios $\varepsilon=5$, the diffraction angles $\xi'=0.1$, 1, 2.5 and 5. From Fig. 6, we can see that the variation of the orientation angle is not monotonous, and there are oscillations for the orientation angle in the near field zone. It is easily found that effects of diffraction angles on the orientation angle are drastic in the near field zone, and variation of the orientation angle with the transmission distance is not obvious when $\xi'=0.1$. What's more, the variation of the orientation angle becomes severe when $\xi'=1$, and it reaches to maximum when $\xi'=5$. At last, changes in the orientation angle become stable with the transmission distance. That is because that the orientation angle is another expression of the degree of polarization, and it will change with the variation of the degree of polarization change.

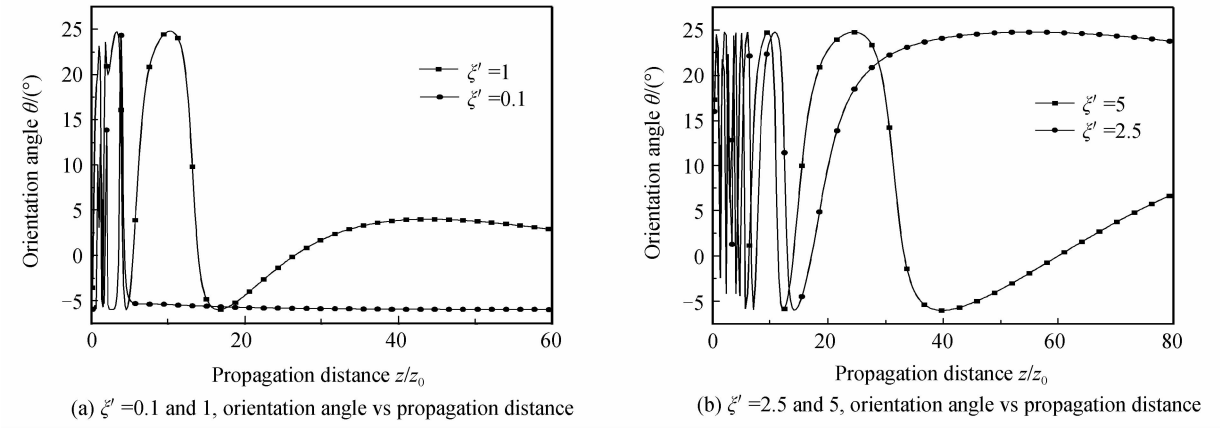

(a) $\xi'=0.1$ and 1, orientation angle vs propagation distance

(b) $\xi'=2.5$ and 5, orientation angle vs propagation distance

Fig. 6 Changes in the orientation angle with the transmission distance in different diffraction angles

2.2.3 Effects of the aperture obscuration ratio and diffraction angle on the degree of ellipticity with the increasing of transmission distance

The numerical results for behaviour of the degree of ellipticity with the transmission distance in different aperture obscuration ratios are given in Fig. 7, where the wavelengths $\lambda=1.06$ μm, the diffraction angle $\xi'=3$, the aperture obscuration ratios $\varepsilon=0.3$, 1, 3 and 5. As shown in Fig. 7, the variation of the degree of ellipticity is not monotonous. The degree of ellipticity exhibits variation with oscillations and the oscillation is stronger for larger aperture obscuration ratios. It is clear that effects of aperture obscuration ratios on the degree of ellipticity are drastic in the near field zone , and the variation of the

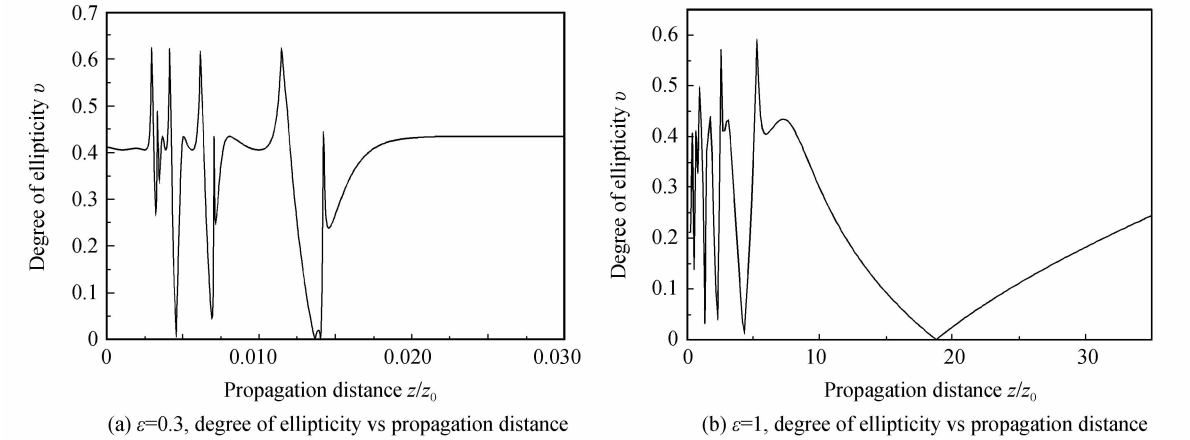

(a) ε=0.3, degree of ellipticity vs propagation distance

(b) ε=1, degree of ellipticity vs propagation distance

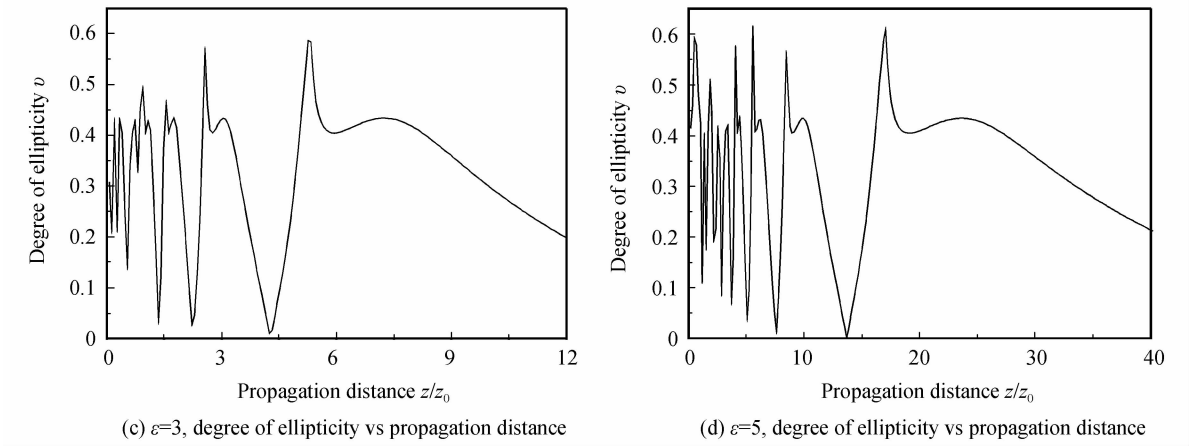

Fig. 7 Changes in the degree of ellipticity with the transmission distance in different aperture obscuration ratios

degree of ellipticity with the transmission distance is not obvious when $\varepsilon=0.3$. Besides, the variation of the degree of ellipticity occurs at $\varepsilon=1$ and it becomes severe with the increasing of aperture obscuration ratio. Furthermore, the variation reaches to maximum when $\varepsilon=5$. At last, with the increasing transmission distance, the degree of ellipticity is uniform and approaches the same value of $\upsilon=0.42$.

The numerical results for behaviour of the degree of ellipticity with the transmission distance in different diffraction angles are shown in Fig. 8, where the wavelength $\lambda=1.06$ μm, the aperture obscuration ratios $\varepsilon=3$, the diffraction angles $\xi'=0.1$, 1, 2.5 and 5. From Fig. 8, we can note that the variation of the degree of ellipticity is not monotonous, and the degree of ellipticity exhibits variation with oscillations, especially in the near field zone. Obviously, effects of diffraction angles on the degree of ellipticity are drastic with the transmission distance in the near field zone, and the degree of ellipticity is basically unchanged with increasing transmission distance when $\xi'=0.1$. It is easy to find that the variation of the orientation angle appears at $\xi'=1$. What's more, the variation becomes severe when $\xi'=2.5$, and it reaches to maximum when $\xi'=5$. And at last, the degree of ellipticity is uniform with the transmission distance.

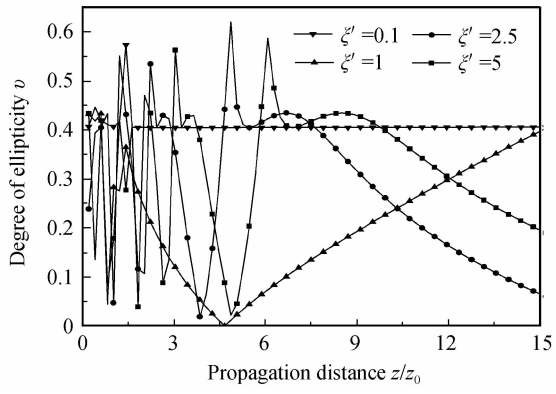

Fig. 8 Changes in the degree of ellipticity with the transmission distance in different diffraction angles

3 Conclusion

According to the extended Huygens-Fresnel principle and Collins formula, based on complex Gaussian function expansion method, the cross-spectral density formula of elliptically polarized GSM passing through the rectangular aperture is derived. Meanwhile, combined the Stokes vector theory, the expressions of light intensity and polarization properties are discussed.

Studies show that effects of the aperture obscuration ratio on light intensity of elliptically polarized GSM passing through the aperture is obvious in the near field zone. It is clear that the variation of the light intensity is not monotonous, and the light intensity exhibits decrement with oscillations in different wavelengths, especially in the near field zone, and the magnitude of variation increases with the increasing wavelength, which depends on the aperture obscuration ratio. Nevertheless, intensity distribution of elliptically polarized GSM is less sensitive to the aperture obscuration ratio and wavelength with the transmission distance in the far-field region.

In addition, effects of the aperture obscuration ratio on polarization properties of elliptically polarized GSM is obvious in the near field zone. It is found that the variation of the degree of polarization, orientation angle and degree of ellipticity are not monotonous, and they exhibit variation with oscillations. Besides, the variation increases with the increasing of the aperture obscuration ratio in different diffraction angles. The magnitude of variation in the degree of polarization, orientation angle and degree of ellipticity increases with the increasing of diffraction angle, which is decided by the aperture obscuration ratio. However, in the far-field region, effects of the aperture obscuration ratio and diffraction angle are not severe, and the behaviour of the degree of polarization, orientation angle and degree of ellipticity over sufficient long distances are

not affected by the aperture obscuration ratio and diffraction angle.

References

[1] LIU Hai-gang, LV Bai-da. Focusing properties of non-uniformly polarized beams through an astigmatic lens with annular aperture[J]. *Acta Optica Sinica*, 2009, **38**(7): 1602-1606.

[2] HAN Yong, WU Jian, YANG Chun-ping, *et al*. Research by the transmission characteristics of the beam through an annular aperture optical system[J]. *Journal of Applied Optics*, 2008, **29**(4): 661-664.

[3] MOHAMED S, EMIL W. Coherence-induced polarization changes in light beams[J]. *Optics Letters*, 2008, **33**(11): 1180-1182.

[4] LIU Chao, LIU Qiang-sheng, CEN Zhao-feng, *et al*. Analysis methods for polarization state and energy transmission of rays passing in optical systems[C]. SPIE, 2010, **7849**: 78490G.

[5] ZHOU Zhe-hai, WANG Xiao-ling, NIU Chun-hui. Focusing properties of high numerical aperture linearly polarized light with axial symmetry[C]. The International Symposium on Test Automation & Instrumentation, 2009, 1:230-233.

[6] PAN Liu-zhan, FENG Jan-wu, DING Chao-liang. On-axis spectral changes of gaussian schell-model beams passing through an astigmatic aperture lens[J]. *Acta Photonica Sinica*, 2007, **36**(8): 1448-1451.

[7] JIA Xin-ting, LI Bo, WANG You-qing. Far-field properties of a cylindrically polarized vector beam and its beam quality beyond the paraxial approximation[J]. *Chinese Optics Letters*, 2010, **8**(5): 517-519.

[8] ZHOU Zhe-hai. Generation, characteristics and applications of axially symmetric polarized beam[D]. Beijing: Tsinghua University, 2010.

[9] ZHANG Guo-wen, PU Ji-xiong. Cross-polarization degree of partially coherent electromagnetic beams propagating in turbulent atmosphere[J]. *Learned Journal of Huaqiao University* (*Natural Science*), 2011, **32**(1): 21-28.

[10] WANG Hai-yan, LI Xiang-yin. Spectral properties of apertured stochastic electromagnetic twist anisotropic Gaussian Schell-model beam passing in turbulent atmosphere[J]. *Optik*, 2011, **122**: 429- 434.

[11] GAO Ming, NAN Wei-na, LÜ Hong. Polarization changes of elliptically polarized laser beams passing in slant path through turbulent atmosphere[J]. *Advanced Materials Research*, 2013, **605- 607**: 1994-1998.

[12] ZHAO Ting-jing. Effects of the aperture on axis polarization properties of the partially coherent beam[J]. *Laser Technology*, 2008, **32**(3): 424-426.

[13] PAN Liu-zhan. Far-field behavior of partially polarized Gaussian Schell-model beams diffracted through an aperture[J]. *Acta Optica Sinica*, 2006, **26**(8): 1250-1255.

[14] XU Bi-jun. Propagation properties of elliptical symmetry anomalous hollow beams through a circular aperture[J]. *Infrared and Laser Engineering*, 2011, **40**(10): 1985-1987.

[15] FU Wen-yu. Effect of the polarization properties of Gaussian Schell-model beams on rectangular[J]. *Optical Technology*, 2008, **34**(4): 528-531.

[16] GAO Ming, NAN Wei-na, LÜ Hong, *et al*. Analysis on influence of the turbulent on polarization properties of elliptically polarized laser beams in propagation[J]. *Acta Photonica Sinica*, 2013, **42**(9): 1107-1111.